

Laser micromachining of goldblack coatings

N. Nelms, J. Dowson, N. Rizvi, and T. Rohr

Goldblack deposits have been used as high-absorption coatings for thermal infrared detectors for a number of years, principally on large single, or few pixel detectors. We present a new technique that allows the benefits of goldblack to be applied to the current generation of small pixel silicon micromachined thermal infrared detectors. © 2006 Optical Society of America

OCIS codes: 040.3060, 160.1890.

1. Introduction

Goldblack coating has been used for a number of years to improve the spectral absorption of thermal infrared detectors.^{1–3} It is a low-density amorphous deposit that can have absorption close to unity over a wide bandwidth from visible to midinfrared wavelengths^{4,5} or even longer.⁶ Goldblack deposition involves the slow evaporation of gold under a low pressure of inert gas (see Section 2), and it is this method that has generally limited its application to large single pixel devices such as pyroelectric detectors.³ The new generation of small pixel (typically tens of μm) silicon micromachined thermal infrared detectors⁷ can equally benefit from the application of gold-black coatings provided that the coating can be applied in a reticulated fashion. Thermally bridging the gap between pixels will lead to unacceptable levels of cross talk. Some success has been achieved using a reticulated mask,⁸ but such depositions are difficult due to the small size of the holes. Also, this method invariably leads to a Gaussian-type profile across the pixel providing nonuniform absorption. Thermal bridging and misalignment due to differential thermal expansion between detector and mask and parallax effects are also common. To overcome these difficulties, we have developed a method whereby goldblack is deposited across the entire pixel area. A laser is then used to remove the coating that

has built up over the gaps between pixels. As part of this work, we have also investigated mask deposition to compare the results with those obtained using the laser.

2. Goldblack Deposition

We have designed and built our own facility for the deposition of high-performance goldblack coatings. The facility is built around a custom stainless-steel vacuum chamber equipped with a rotary-backed turbomolecular pump and is capable of reaching pressures of the order of 10^{-7} mbar (Fig. 1). Precise control of key parameters including chamber pressure, substrate temperature, and evaporation current is available and provides repeatable production of goldblack coatings with high absorption (see Fig. 2). A fuller description of the facility, goldblack deposition procedure, and the performance of the bulk coating have been recently reported.⁵ However, for clarity, a typical deposition run is described below:

- Install substrate and gold metal.
- Evacuate chamber (min. 12 h).
- Cool substrate (-55 °C).
- Set chamber pressure (10 mbar).
- Let substrate temperature stabilize (15 min).
- Melt gold metal, hold for 60 s (typical current 75–80 A).
- Increase current slowly to evaporation level (typically 80–90 A).
- Allow gold to fully evaporate (typically 100 s).
- Warm up substrate.
- Vent chamber to dry N_2 .

The gold metal is 99.99+% pure in the form of 0.5 mm diameter wire. The chamber is pumped for 12 h to reduce residual water content in the chamber.

N. Nelms (nin@star.le.ac.uk) and J. Dowson are with the Space Research Centre, University of Leicester, Leicester LE1 7RH, U.K. N. Rizvi is with IBMM Laser Micromachining Centre, University of Wales Bangor, Bangor LL57 1UT, U.K. T. Rohr is with the Materials and Process Division, European Space Agency—ESTEC, Keplerlaan 1, Noordwijk ZH 2200 AG, The Netherlands.

Received 6 April 2006; revised 16 May 2006; accepted 16 May 2006; posted 17 May 2006 (Doc. ID 69758).

0003-6935/06/276977-05\$15.00/0

© 2006 Optical Society of America

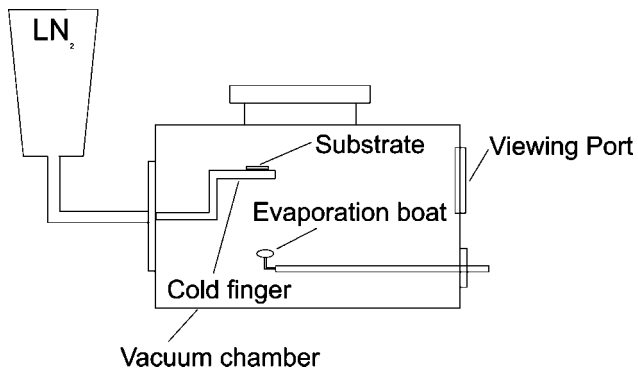


Fig. 1. Goldblack deposition facility. The evaporation boat to cold-finger distance is of the order of 100 mm. Note that the substrate is shielded from direct sight of the boat to avoid heating of the deposit.

3. Coating of Small Pixel Detectors

Figure 3(a) is a schematic of the 256 pixel linear thermoelectric array that was used for the work described in this paper. It is manufactured by Honeywell and has characteristics as presented in Table 1. The detector is a silicon micromachined structure with pixels suspended over a deep open trench by silicon nitride legs [see Fig. 3(b)]. For deposition, the detector is placed on a copper block and held between a fixed peg and a spring-loaded peg. Figure 4(a) shows part of a detector prior to deposition. A strip of goldblack is then deposited along the entire array [Fig. 4(b)]. This is achieved by using a slit mask located above the detector during the deposition process. The slit mask is made from beryllium copper and has dimensions of 24×14 mm. In the center is a uniform slit with a length of 15 mm and a width of $90 \mu\text{m}$. The mask is glued into a stainless-steel frame. The mask-frame assembly is then placed over the detector on the copper block and aligned. Alignment is achieved using an optical microscope in combination with a custom 3D translation stage. This allows very precise positioning of the slit above the detector pixel area (of the order of $1 \mu\text{m}$). The target thickness of the goldblack coating is $20\text{--}40 \mu\text{m}$, and the detector-mask separation distance is an impor-

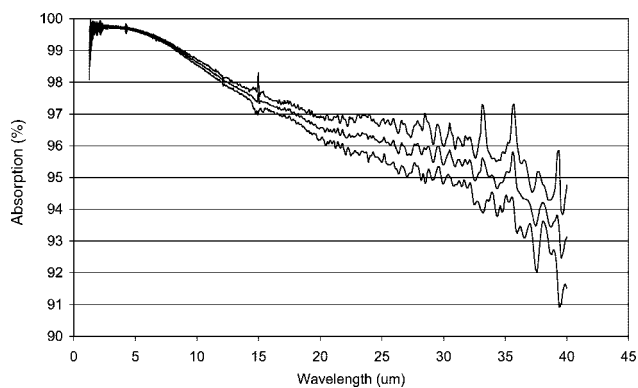
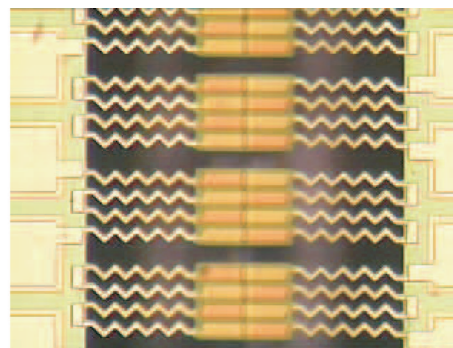
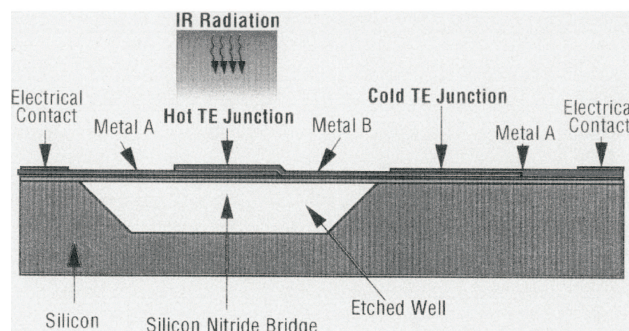


Fig. 2. Mean absorption response for a number of goldblack coatings plotted with $\pm 1\sigma$.



(a)



(b)

Fig. 3. (Color online) Detector arrangement. The detector is a linear array with 256 pixels. (a) Pixel active area is $55 \times 45 \mu\text{m}$, each with four linked thermocouples, (b) cross section of array.

tant parameter in achieving this. A number of tests were performed to optimize this distance at $90 \mu\text{m}$. The thickness of the stainless-steel frame was then adjusted to ensure that the correct separation is obtained. Once the mask assembly is aligned above the detector, it is held in place with small applications of quick-drying adhesive in the four corners (Fig. 5). The copper block with the detector and mask assembly is then mounted onto the cold finger inside the vacuum chamber and subjected to a goldblack deposition run as previously described.

4. Laser Micromachining

Using the method described in Section 3, we can make repeatable depositions resulting in a neat strip of goldblack with a typical thickness of $25\text{--}35 \mu\text{m}$ with a smooth profile moving from thinner near the ends to thicker in the middle. This leaves un-

Table 1. Detector Parameters

Parameter	
Number of pixels	256
Pixel size	$45 \mu\text{m} \times 55 \mu\text{m}$
Pixel pitch	$55 \mu\text{m}$
Fill factor	82%
Impedance	$\sim 1200 \Omega$
Responsivity	300 V/W
Time constant	$\sim 4 \text{ ms}$

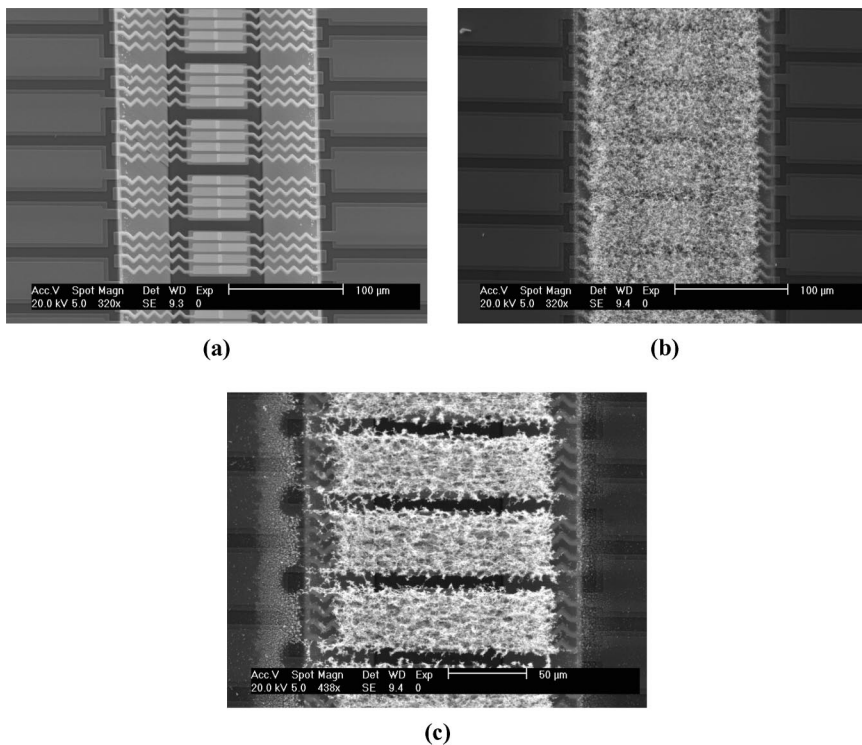


Fig. 4. Detector pixel structures (a) prior to deposition, (b) after strip deposition, and finally (c) postlaser micromachining using a femtosecond laser. Pixel dimensions are $45 \times 55 \mu\text{m}$.

wanted goldblack bridging the gap between adjacent pixels [see Fig. 4(b)]. The distance between the pixels is $10 \mu\text{m}$ and, to remove the bridging deposit, a femtosecond laser micromachining system is used. The system uses a Spectra-Physics Hurricane laser, which outputs pulses of ~ 130 fs duration at a pulse repetition rate of 5 kHz at a wavelength of 800 nm. The detector die is placed on XYZ θ Concentrator

stages, which can be moved and controlled with a resolution of $1 \mu\text{m}$ in the XYZ directions (with the Z movement adjusting the focal position of the laser beam). High-resolution alignment and viewing CCD cameras enable the position of the die to be measured and controlled with respect to the laser beam, allowing for the precise machining of the goldblack coatings. The laser beam was focused onto the die using a singlet silica focusing lens of 75 mm focal length. To determine the optimum processing conditions for the consistent and reproducible removal of the goldblack coating from the die, a series of trials were conducted where varying powers of the laser were used with the die being moved under the focused laser beam at different speeds. Using this approach, it was found that the goldblack coating was best machined at a laser energy density of $0.5 \text{ mJ}/\text{cm}^2$ using two shots per area. The low-energy density is also important to ensure that the detector substrate underneath the goldblack coating is not damaged during the ablation process where material is removed from the detector itself. A number of trials were also performed to verify this. Having found this stable process, each detector was rotationally aligned in the machining tool such that parallel laser cuts could be made in the gaps between each pixel and the detector array was machined [Figure 4(c)]. In a separate test, a UV excimer laser operating at a wavelength of 248 nm was also used to machine goldblack coatings. Using the excimer laser, it was found that a large area (few tens to hundreds of micrometers) surrounding the exposure site was also disturbed or removed, even at very modest ablation energy densities of a few mJ/cm^2 . This was probably attributable to the ablation shock

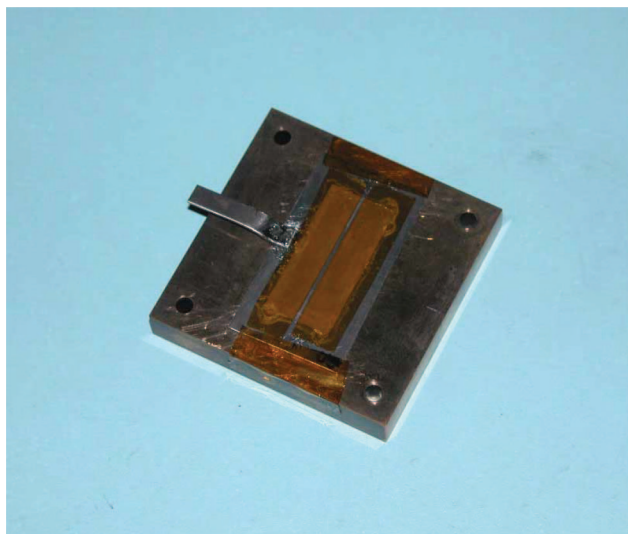


Fig. 5. (Color online) Cold finger with mask and mask-support structure mounted above the detector prior to installation in the deposition facility. The copper cold finger is $40 \times 40 \text{ mm}$. The handle couples to a custom alignment jig. Once alignment is complete, the mask is fixed using small applications of quick-drying adhesive in the corners.

produced when the nanosecond pulses from the excimer laser impacted on the goldblack coating and substrate. No stable machining process could be found for the clean removal of $\sim 10\ \mu\text{m}$ wide tracks in the goldblack coating with the excimer laser, which is why the femtosecond laser machining solution was sought.

5. Spectral Performance

The spectral absorption of the goldblack has been well investigated and is reported in Ref. 5. The aim of the spectral performance measurements in this case was (a) to determine whether the high absorption of the bulk coating is retained when applied to small pixel detectors and micromachined with a laser and (b) to investigate the spatial uniformity of the coating across a micromachined area (a pixel). Reflectance measurements were made since it is not possible to make independent absorption measurements of coated pixels. In previous cases where a total reflectance measurement has been made, the absorption has been assumed to be equal to $1 - \text{reflectance}$. In this case all measurements were made using a Bruker Equinox 55 Fourier transform infrared (FTIR) spectrometer in conjunction with an attached Hyperion 3000 microscope and $15\times$ objective. Surface reflectance profiles were recorded using a 64×64 pixel mercury cadmium telluride (MCT) focal plane array detector and spot reflectance measurements made using a midband MCT detector. This does not provide a true total reflectance measurement and so the plots here are of reflectance rather than absorption. However, this provides a good basis for comparison between samples and to first approximation the absorption can still be calculated from $1 - \text{reflectance}$. The wavelength range of the measurements was $2.5\text{--}15\ \mu\text{m}$ (the limits of the microscope). A gold-coated first surface mirror was used as the background. Measurements were made on uncoated and goldblack-coated detectors. For comparison, coated detectors were produced in two different ways, using a reticulated mask as in previous attempts and using the new strip deposit–laser ablation method described here. Figure 6 shows spot reflectance measurements for all three coating variations (none, reticulated, and laser ablated) with the spot size equal to the whole pixel area ($55 \times 45\ \mu\text{m}$). There is a large difference in reflectance between uncoated and coated detectors as might be expected. There is also a significant improvement in reflectance (of the order of 2%) at the longer wavelengths for the laser-etched coating over the reticulated mask version. The variation in reflectance across the pixels was also studied, using a spot size substantially smaller than the pixel measured with the FPA detector leading to a $4\ \mu\text{m}$ lateral resolution. Figure 7 shows the results (integrated over a $2.5\text{--}11\ \mu\text{m}$ wavelength) along the length of the array that gives a clear indication of the reflectance profile across the pixel and the interpixel gaps. Figure 7(a) is for the uncoated array and provides the reference point for the two coated arrays. To be clear, the plots

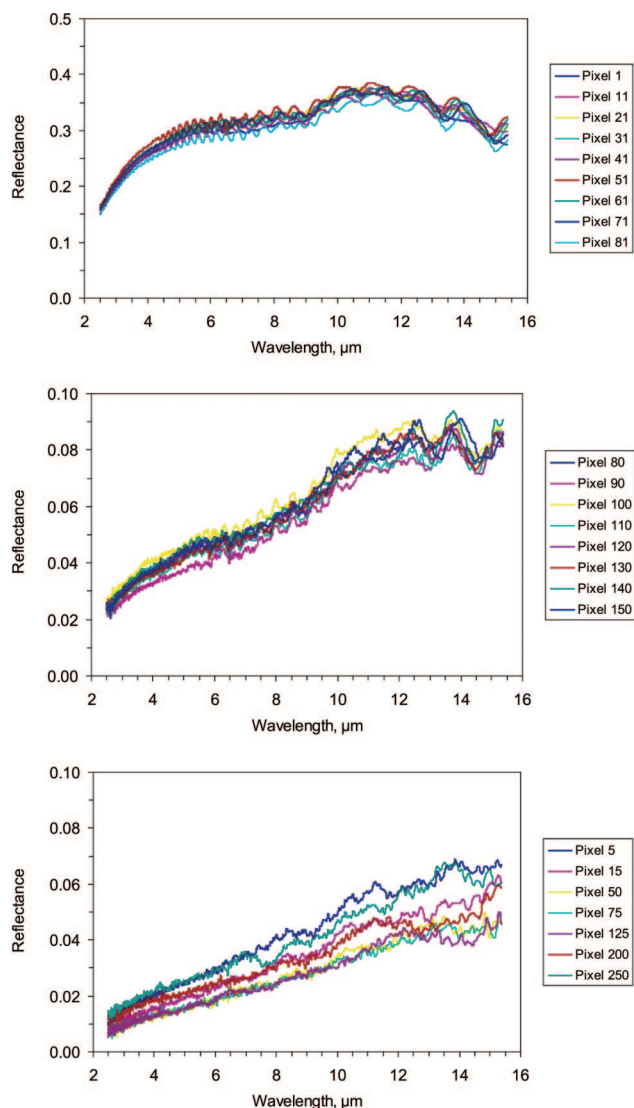


Fig. 6. (Color online) Spot reflectance measurements for uncoated (top), reticulated mask (middle), and laser-machined goldblack (bottom) -coated pixels. Each plot shows measurements from eight pixels across the array. Note the change of scale for the bottom plot.

are again reflectance ($\sim 1 - \text{absorption}$), and so for the uncoated pixels the absorption is less than that of the interpixel gap, which has an apparent reflectance of the order of 15%. Figure 7(b) shows the results for the pixel coated using the reticulated mask. It is obvious now that the pixel absorption is greater than the interpixel gap. However, what is also clear is that the goldblack has a smooth Gaussian-type profile, indicated by the decrease in reflectance toward the center of the pixel where the coating reaches the desired thickness. Compare this with the results shown in Fig. 7(c) which, due to the laser micromachining, has a much squarer profile indicating a more uniform deposition across the surface of the pixel. This in turn contributes to a higher overall detector efficiency and a more predictable response. The square profile is also likely to be responsible for the

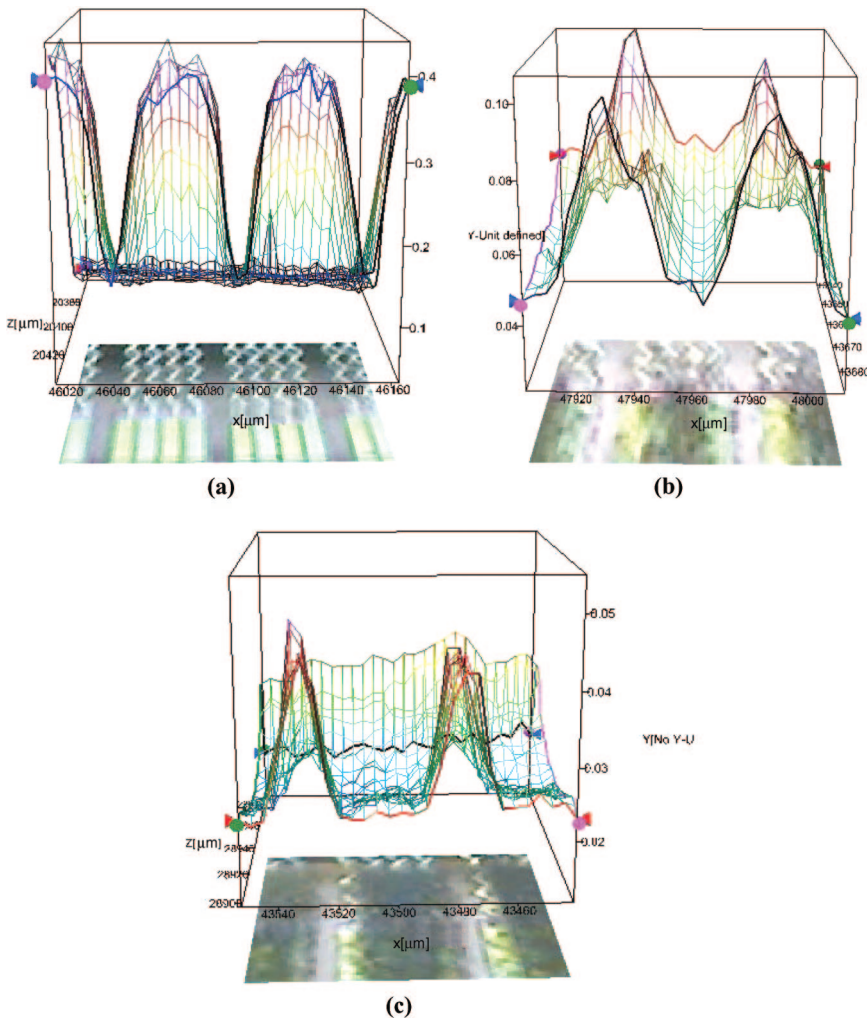


Fig. 7. (Color online) Reflectance (integrated over 2.5–11 μm wavelength) profile across the detector for (a) uncoated pixels, (b) goldblack-coated pixels using reticulated mask deposition, and (c) goldblack-coated pixels using strip deposition and lasermicro-machining.

2% improvement in overall pixel absorptance over the reticulated mask coating mentioned since the coating remains the correct thickness to the edge of the pixel.

6. Conclusions

Goldblack coatings provide an effective means of improving the response and spectral flatness of thermal infrared detectors. To date, there has been difficulty in applying such coatings to small pixel detectors. Femtosecond laser ablation has been demonstrated as a highly suitable and practical way of machining delicate goldblack detector coatings without causing damage to the underlying substrate. For thermal infrared detectors, it provides a method of creating a uniform, isolated deposit on small pixel structures that is not achievable using a reticulated mask technique.

The authors thank E. Theocarous of the National Physical Laboratory, Teddington for many useful discussions, and C. Borrero for her efforts in the method development for infrared reflectance.

References

1. W. R. Blevin and J. Geist, "Influence of black coatings on pyroelectric detectors," *Appl. Opt.* **13**, 1171–1178 (1974).
2. W. Becker, R. Fettig, A. Gaymann, and W. Ruppel, "Black gold deposits as absorbers of far infrared radiation," *Phys. Status Solidi B* **194**, 241–255 (1996).
3. J. Lehman, E. Theocarous, G. Eppeldauer, and C. Pannell, "Gold-black coatings for freestanding pyroelectric detectors," *Meas. Sci. Technol.* **14**, 916–922 (2003).
4. D. J. Advena, V. T. Bly, and J. T. Cox, "Deposition and characterization of far-infrared absorbing gold black films," *Appl. Opt.* **32**, 1136–1144 (1993).
5. N. Nelms and J. Dowson, "Goldblack coating for thermal infrared detectors," *Sens. Actuators A* **120**, 403–407 (2005).
6. W. Becker, R. Fettig, and W. Ruppel, "Optical and electrical properties of black gold layers in the far infrared," *Inf. Phys. Technol.* **40**, 431–445 (1999).
7. J. L. Tissot, "Advanced IR detector technology development at CEA/LETI," *Inf. Phys. Technol.* **43**, 223–228 (2002).
8. N. Nelms, G. Butcher, O. Blake, R. Cole, C. Whitford, and A. Holland, "The IR detector system for the GERB instrument," in *Proceedings of the NASA Thermal Detector Workshop* (NASA, 2003), <http://www-lep.gsfc.nasa.gov/code693/tdw03/proceedings/start.html>.